Non-Linear Analysis of Sudden 3-Phase Short-Circuit in a Synchronous Generator

By

Yoshiaki INOUE*, Yoshisuke UEDA* and Chikasa UENOSONO**

(Received September 27, 1983)

Abstract

The present paper investigates the saturation effect on a sudden 3-phase short-circuit which occurs in a salient-pole synchronous generator used in Kyoto University's model power transmission system. Since the magnetic saturation occurs primarily in the pole-core of the machine, the saturation is taken into account in deriving the direct-axis equivalent circuit. First, we make a direct-axis saturation model and then, based upon it, derive a differential equation which regulates flux-linkages under a sudden 3-phase short-circuit condition. With the same degree of accuracy as in the conventional linear theory, this equation can be separated into a set of linear equations which can regulate the armature flux-linkages, and a non-linear differential equation which can regulate the field flux-linkage. By means of such theoretical considerations, simulations and experiments, we clarify how the saturation effects both the amplitudes and the time-constants of the alternating- and the direct-current components of short-circuit currents.

1. Introduction

In the analysis of electric power system stability, it is critically important that the effect of magnetic saturation is taken into account in evaluating the dynamic performance of synchronous generators. As is well known, the problem of the saturation effect in synchronous generators is both an old and modern one. From the 1920's up until today, a great amount of literature about the problem has been published. Much of it has dealt with either one or the other of the following two subjects: (1) how to measure and calculate saturated reactances[1] and (2) how to construct mathematical models of saturated machines[2]. It may seem that very little attention has been paid as to how saturation effects the individual performance of synchronous generators (e.g. sudden 3-phase short-circuit, etc.). Such an investigation is also required for a thorough understanding of the saturation effect.

This paper describes a non-linear analysis of a sudden 3-phase short-circuit

* Department of Electrical Engineering, II.
** Emeritus professor of Kyoto University.

which occurs in a salient-pole 6kVA micro-generator. The machine is used as a water-wheel generator in Kyoto University's model power transmission system. In the present paper, magnetic saturation is taken into account in deriving a direct-axis equivalent circuit, because the saturation occurs primarily in the pole-core of the machine. In the following, first we discuss a direct-axis saturation model and then derive a non-linear differential equation which regulates flux-linkages under a sudden 3-phase short-circuit condition. Then, by both simulations and experiments, the saturation effect upon a short-circuit current is investigated.

T_d'' of the experimental machine is 12 ms. It is too short to accurately observe the saturation effect in a subtransient condition. Hence, in the present paper, dumper-windings are prescribed to be an open-circuit. The saturation effect in the subtransient condition will be discussed at another time.

2. Direct- and Quadrature-Axis Magnetic Characteristics of the Experimental Machine

The experimental machine is a 4-pole and salient-pole type synchronous

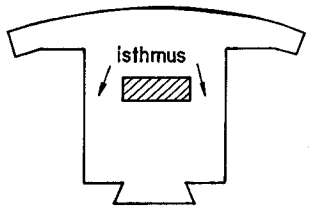

Fig. 1. Construction of the field-core.

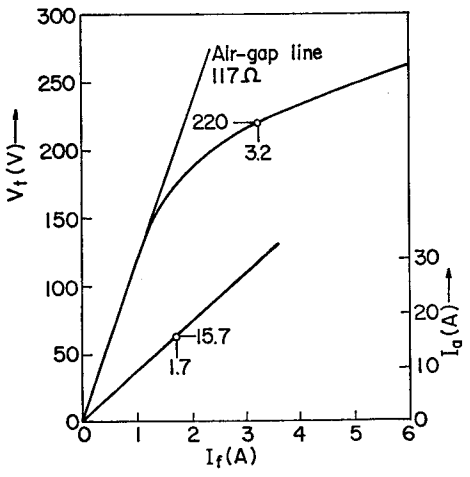

Fig. 2. No-load saturation curve and short-circuit curve.

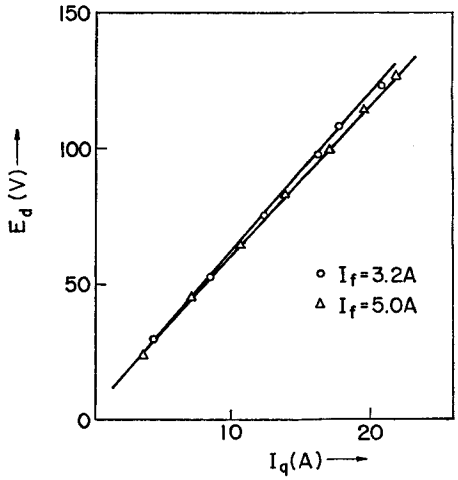

Fig. 3. Quadrature-axis current I_q vs. direct-axis voltage E_d.

generator. Its rated capacity, voltage and current are 6kVA, 220V and 15.7A respectively[3,4]. The machine is equipped with an isthmus pole (see Fig. 1) to fit its no-load saturation curve (Fig. 2) to that of an actual 13MVA machine.

Generally speaking, direct- and quadrature-axis magnetic characteristics are represented by a no-load saturation curve (Fig. 2) and I_q vs. E_d curves (Fig. 3) respectively. As Fig. 3 shows, I_q vs. E_d relations are almost straight-line, and their slopes scarcely depend upon field currents. Thus, from Fig. 2 and Fig. 3, it may be concluded that the direct- and the quadrature-axis circuits of the machine are independent of each other, and only the direct-axis circuit is influenced by the magnetic saturation.

The field current necessary to induce the rated voltage on no load is 3.2A, and the current necessary on the rated load is 5.0A.

3. Derivation of Direct-Axis Saturation Model and Saturated Reactances

3-1. Direct-axis Saturation Model

Eqs.(9) and (12) of the present paper, the former giving the saturated x_d and the latter clarifying the relationship between x_d' and x_p, may be found in other reports[3,4]. However, when magnetic saturation occurs primarily in pole-core, the above two equations can be obtained more easily than the complicated discussions in the reports suggest. The method of derivation which we present is advantageous in that it allows an easy understanding of the physical meaning of the Potier triangle and the Potier reactance.

Here, we consider the unsaturated direct-axis circuit. The field flux-linkage ψ_f and the armature flux-linkage ψ_d are given by

$$\left.\begin{aligned}\psi_f &= L_{fu}I_f + L_{mdu}I_d \\ \psi_d &= L_{mdu}I_f + L_{du}I_d\end{aligned}\right\} \tag{1}$$

(Suffix u denotes an unsaturated value.)

L_{fu}, L_{mdu} and L_{du} of the experimental machine are listed in Table 1. Let's denote the ratio of L_{mdu} to L_{fu} and that of L_{du} to L_{mdu} by k and k_s respectively. That is,

Table 1. L_{fu}, L_{mdu} and L_{du} of the experimental machin

	measured value	method of measurement
L_{fu}	6.8H	extrapolation of the frequency-response curve of field-winding's impedance.
L_{mdu}	0.31H	slope of the air-gap line of no-load saturation curve.
L_{du}	0.020H (94%)	Slip-test.

$$k=\frac{L_{mdu}}{L_{fu}}\left(=\frac{0.31}{6.8}=0.046\right),\quad k_s=\frac{L_{du}}{L_{mdu}}\left(=\frac{0.020}{0.31}=0.065\right) \tag{2}$$

The values in parenthesis are of the experimental machine. Using the above k and k_s, Eq.(1) can be transformed into

$$\left.\begin{aligned} k\psi_f&=kL_{mdu}(I_f/k+I_d)\\ \psi_d&=k\psi_f+L_{mdu}(k_s-k)I_d \end{aligned}\right\} \tag{3}$$

The implication of Eq.(3) can be illustrated by the equivalent circuit of Fig. 4, where L_p is given by

$$L_p=L_{mdu}(k_s-k)\quad(=6\,\mathrm{mH}=29\%) \tag{4}$$

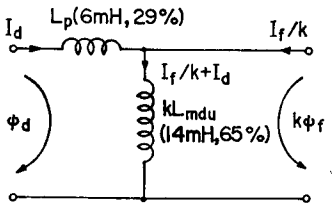

Fig. 4. Unsaturated direct-axis equivalent circuit.

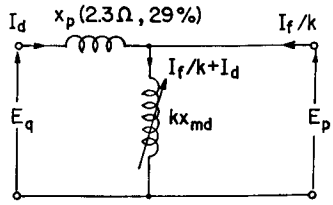

Fig. 5. Saturated direct-axis equivalent circuit.

Now, as the direct-axis magnetic saturation depends on the field flux-linkage, the saturated direct-axis equivalent circuit of Fig. 5 may be deduced from Fig. 4. In Fig. 5, voltages are used instead of flux-linkages, and x_p is given by

$$x_p=x_{mdu}(k_s-k)\quad(=2.3\Omega=29\%) \tag{5}$$

Inspection of Fig. 5 leads to the following 1°～4°.

1° Field MMF is given by $I_f/k+I_d$ or I_f+kI_d, and the direct-axis saturation

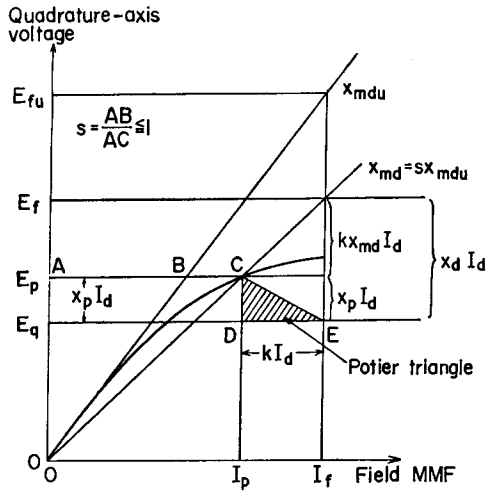

Fig. 6. Graphical evaluation of saturated reactances.

is represented by the relationship between x_{md} and I_f+kI_d. From now on, we will denote field MMF by I_p, that is, $I_p=I_f+kI_d$.

2° E_p in Fig. 5 is given as the no-load voltage induced when the field current would be equal to I_p (see Fig. 6).

3° Quadrature-voltage E_q is given by $E_q=E_p+x_pI_d$.

4° Since the values of k and x_p don't depend on the saturation, they are constant.

The above 1°~4° can be interpreted graphically as Fig. 6. △CDE is the so called Potier triangle, and it depends not on I_f but on I_d. Consequently, x_p defined by Eq.(5) is the Potier reactance, and E_p in Fig. 5 and Fig. 6 corresponds to the voltage behind the Potier reactance.

In the above discussions, we have obtained the values of k and x_p from the unsaturated values of L_f, L_{md} and L_d. (See Eq.(2) and Eq.(5).) Usually, k and x_p are obtained by actually drawing a Potier triangle with both a no-load saturation curve and a zero p.f. saturation curve. The values obtained by the two methods are compared in Table 2. They agree well with each other. This proves the validity of the discussions so far.

Table 2. k and x_p obtained by two method

	by Eq. (2) and Eq. (5)	by drawing a Potier triangle
k	0.046	0.045
x_p	2.3Ω (29%)	2.4Ω (30%)

3-2. Saturated Reactances

Based upon the diagram in Fig. 6, let's derive analytical expressions of saturated x_{md}, x_f and x_d. The saturated x_{md} is presented by the slope of line OC in Fig. 6. Thus, defining saturation factor s as

$$s=AB/AC \quad (\leqq 1) \tag{6}$$

x_{md} is given by

$$x_{md}=sx_{mdu} \tag{7}$$

Dividing every member of Eq.(7) by k yields the saturated x_f, that is,

$$x_f=sx_{fu} \tag{8}$$

Under this saturated condition, the field-current I_f induces a voltage E_f or $x_{md}I_f$ in the armature winding. (See Fig. 6.) Hence, the voltage drop from E_f to E_q is due to the direct-axis armature reaction which must be equal to x_dI_d. From this we obtain the saturated x_d as

$$x_d=x_p+skx_{mdu}=x_p+s(x_{du}-x_p) \tag{9}$$

where x_p is given by Eq.(5). After all, with the saturation factor s determined by the voltage behind the Potier reactance E_p or the field MMF I_p, the saturated

x_{md}, x_f and x_d can be calculated by Eq.(7), Eq.(8) and Eq.(9) respectively.

We can present another form of expression for x_d instead of Eq.(9). By inspecting Fig. 6, we obtain the following equations,

$$E_p=E_q-x_pI_d,\ E_f=E_q-x_dI_d,\ E_p/E_f=(I_f+kI_d)/I_f \tag{10}$$

and eliminating E_p and E_f from them yields

$$x_d=\frac{E_q+x_pI_f/k}{I_f/k+I_d}. \tag{11}$$

Eq.(11) makes it possible to calculate the saturated x_d with quantities to be measured at the generator's terminal-side such as the line-voltage V_t, current I_t, rotor-angle δ and load-angle φ. That is, after calculating E_q and I_d by $E_q=V_t\cos\delta$ and $I_d=\sqrt{3}I_t\sin(\delta+\varphi)$, we can obtain the saturated x_d by substituting them into Eq.(11).

The thin line in Fig. 7 shows the I_p vs. s characteristic of the experimental machine calculated from the no-load saturation curve (Fig. 2). The thick line in the figure shows x_d evaluated by Eq.(9). From the unsaturated value of 94% (=7.6Ω), x_d decreases gradually as I_p increases, and it is 65% and 56% at I_p=3.2A and 5.0A respectively. The circles in the figure show the results calculated by Eq.(11). Both x_d's agree with each other. Therefore, the x_d obtained here is proved to be valid.

According to the equivalent circuit in Fig. 5, the direct-axis transient reactance x'_d is given by

$$x'_d=x_p\ (=2.3\Omega=29\%) \tag{12}$$

and so it is independent of saturation. The value of x'_d measured by the Dalton-Cameron method is also 2.3Ω and it agrees with the value given in Eq.(12). In Fig. 5, the field-flux saturation, not the armature leakage-flux saturation, is considered. Because a very large armature-current flows in the sudden 3-phose short-circuit condition, saturation in the armature leakage-flux may occur. Hence, the value of x'_d may be a little less than the value given above. Fig. 8 shows x'_d

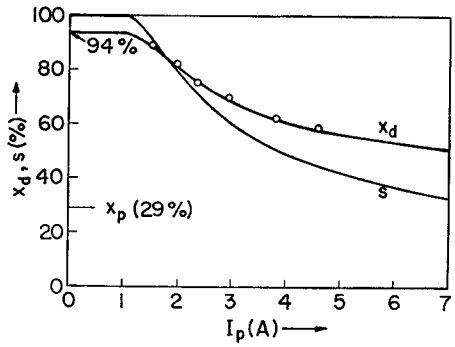

Fig. 7. I_p vs. s characteristic and saturated x_d.

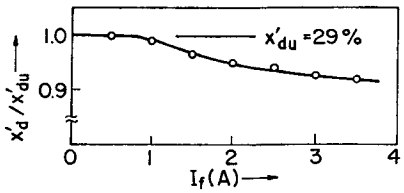

Fig. 8. Saturated x_d'.

obtained by actual sudden 3-phase short-circuit experiments. The value of x'_d at $I_f=3.2$A (the line-voltage before the short-circuit is the rated one or 220V) is about 8% less than its unsaturated value. Strictly speaking, an analytical expression like Eq.(9) must also be introduced for x'_d. However, because an analytical estimation of the armature leakage-flux saturation is difficult in the present situation, and since the range of variation of x'_d is relatively small, this paper approximates x'_d as follows. That is, x'_d is assumed to depend only on the field-current I_f before the short-circuit and to be invariant during the transient period. The value is given by Fig. 8. As illustrated later, this approximation does not lead to serious error.

4. Generator Equation Featuring Flux-Linkages in the Sudden 3-Phase Short-Circuit Condition

Park's equation of a synchronous generator without a dumper winding is given by[5]

$$\left.\begin{aligned}
&\frac{d\psi_d}{dt}=-v_d-\psi_q\omega-r_a i_d\,;\ \psi_d=L_d i_d+L_{md}i_f\\
&\frac{d\psi_q}{dt}=-v_q+\psi_d\omega-r_a i_q\,;\ \psi_q=L_q i_q\\
&\frac{d\psi_f}{dt}=E_f-r_f i_f\qquad\ ;\ \psi_f=L_{md}i_d+L_f i_f
\end{aligned}\right\}\tag{13}$$

where $v_d=v_q=0$ in the short-circuit condition. L_d, L_{md} and L_f in the equation are given by expressions exactly similar to x_d, x_{md} and x_f respectively. (See Eq.(7) ~ Eq.(9).) That is,

$$L_d=L_p+s(L_{du}-L_p),\ L_{md}=sL_{mdu},\ L_f=sL_{fu}\tag{14}$$

where s is determined by i_p or i_f+ki_d. (See Fig. 6 and Eq.(6).)

To make it possible to easily understand the effect of the magnetic saturation, Eq.(13) may be rewritten to contain only the flux-linkages ψ_d, ψ_q and ψ_f as follows:

$$\frac{d}{dt}\begin{pmatrix}\psi_d\\ \psi_q\\ \psi_f\end{pmatrix}=\begin{pmatrix}-\dfrac{r_a}{L'_d} & -\omega & \dfrac{kr_a}{L'_d}\\ \omega & -\dfrac{r_a}{L_q} & 0\\ \dfrac{kr_f}{L'_d} & 0 & -\dfrac{r_fL_d}{L_fL'_d}\end{pmatrix}\begin{pmatrix}\psi_d\\ \psi_q\\ \psi_f\end{pmatrix}+\begin{pmatrix}0\\ 0\\ E_f\end{pmatrix}\tag{15}$$

The currents i_d, i_q and i_f are determined by

$$\begin{pmatrix}i_d\\ i_q\\ i_f\end{pmatrix}=\begin{pmatrix}\dfrac{1}{L'_d} & 0 & -\dfrac{k}{L'_d}\\ 0 & \dfrac{1}{L_q} & 0\\ -\dfrac{k}{L'_d} & 0 & \dfrac{L_d}{L_fL'_d}\end{pmatrix}\begin{pmatrix}\psi_d\\ \psi_q\\ \psi_f\end{pmatrix}\tag{16}$$

Because L'_d is assumed to be invariant during the transient period, only the two (3, 3) elements of the coefficient matrices of Eq.(15) and Eq.(16), i.e. $-r_f L_d / L_f L'_d$ and $L_d / L_f L'_d$, vary with i_p or $i_f + k i_d$. The other elements of the matrices are constant.

Now, when we refer to the conventional linear analysis of the sudden 3-phase short-circuit[5], an approximate solution may be obtained on the assumption that r_a and $r_f \ll 1$ because of the difficulty in obtaining its exact solution. If we adopt the same approximation in our analysis, we can solve Eq.(15) by ignoring the (1, 3) and (3, 1) elements of the right-hand side coefficient matrix. Consequently, with the same degree of accuracy as in the conventional linear analysis, we can separate Eq.(15) into sets of linear and non-linear differential equations. The former, which regulates the armature flux-linkages ψ_d and ψ_q is

$$\frac{d}{dt}\begin{pmatrix}\psi_d\\ \psi_q\end{pmatrix}=\begin{pmatrix}-\dfrac{r_a}{L'_d} & -\omega\\ \omega & -\dfrac{r_a}{L_q}\end{pmatrix}\begin{pmatrix}\psi_d\\ \psi_q\end{pmatrix} \tag{17}$$

and the latter, which regulates the field flux-linkage ψ_f is

$$\frac{d\psi_f}{dt}=-f(\psi_f)+E_f, \quad \text{where } f(\psi_f)=\frac{r_f L_d}{L_f L'_d}\psi_f \tag{18}$$

With respect to the non-linear term $f(\psi_f)$, see Fig. 14. After all, the analysis of the sudden 3-phase short-circuit results in solving Eq.(17) and Eq.(18) under the initial condition that

$$\begin{pmatrix}\psi_d\\ \psi_q\\ \psi_f\end{pmatrix}=\begin{pmatrix}L_{md}I_f\\ 0\\ L_f I_f\end{pmatrix}=\begin{pmatrix}E_0/\omega\\ 0\\ E_0/k\omega\end{pmatrix} \tag{19}$$

where I_f and E_0 are the field-current and the line-voltage before the short-circuit. After ψ_d, ψ_q and ψ_f are obtained, i_d, i_q and i_f can be calculated by Eq.(16).

5. Transient Currents on the Sudden 3-Phase Short-Circuit

5-1. Current Solutions of the Generator Equation

As mentioned above, the generator equation for the sudden 3-phase short-circuit is composed of two parts i.e. Eq.(17) and Eq.(18). Since Eq.(17), which dominates ψ_d and ψ_q, is a linear differential equation, it can be solved easily. Referring to the initial condition Eq.(19), the solution is given by

$$\left.\begin{aligned}&\begin{pmatrix}\psi_d\\ \psi_q\end{pmatrix}=\Psi_a(t)\begin{pmatrix}\cos\omega t\\ \sin\omega t\end{pmatrix},\\ &\text{where, } \Psi_a(t)=(E_0/\omega)e^{-t/T_a}\\ &\qquad T_a=1\Big/\Big[\frac{r_a}{2}\Big(\frac{1}{L'_d}+\frac{1}{L_q}\Big)\Big]\end{aligned}\right\} \tag{20}$$

T_a is the so called armature time-constant. On the other hand, Eq.(18), which dominates ψ_f, is a non-linear differential equation, and so it is difficult to solve. Tentatively, we denote the solution by*

$$\psi_f=\Psi_f(t) \tag{21}$$

The property of $\Psi_f(t)$ will be discussed in section 5-3.

Substituting the above ψ_d, ψ_q and ψ_f into Eq.(16) yields the current solutions of i_d, i_q and i_f. The armature phase-current is also obtained from i_d and i_q. The results are

$$\left.\begin{aligned} i_a&=\sqrt{\frac{2}{3}}\,\frac{1}{2}\left(\frac{1}{L'_d}+\frac{1}{L_q}\right)\Psi_a(t)\cos\alpha-\sqrt{\frac{2}{3}}\,\frac{k}{L'_d}\Psi_f(t)\cos(\omega t+\alpha)\\ i_f&=-\frac{k}{L'_d}\Psi_a(t)\cos\omega t+\frac{L_d}{L_fL'_d}\Psi_f(t)\end{aligned}\right\} \tag{22}$$

where α is the rotor-position at the instant of the short-circuit. The second harmonic in i_a is ignored because it is small.

Let's represent i_a and i_f where their direct-current and alternating-current components are separated from each other. That is,

$$\left.\begin{aligned} i_a&=I_a^{DC}(t)\cos\alpha-\sqrt{2}\,I_a^{AC}(t)\cos(\omega t+\alpha)\\ i_f&=-I_f^{AC}(t)\cos\omega t+I_f^{DC}(t)\end{aligned}\right\} \tag{23}$$

As shown by the above equation, the transient states of i_a and i_f are characterized by those of $I_a^{DC}(t)$, $I_a^{AC}(t)$, $I_f^{AC}(t)$ and $I_f^{DC}(t)$. From Eq.(22) and Eq.(23), we obtain

$$\left.\begin{aligned} &I_a^{DC}(t)=\sqrt{\frac{2}{3}}\,\frac{1}{2}\left(\frac{1}{L'_d}+\frac{1}{L_q}\right)\Psi_a(t),\quad I_a^{AC}(t)=\frac{1}{\sqrt{3}}\,\frac{k}{L'_d}\Psi_f(t)\\ &I_f^{AC}(t)=\frac{k}{L'_d}\Psi_a(t)\qquad\qquad\qquad,\quad I_f^{DC}(t)=\frac{L_d}{L_fL'_d}\Psi_f(t)\end{aligned}\right\} \tag{24}$$

As represented by Eq.(24), the transients of $I_a^{DC}(t)$ and $I_f^{AC}(t)$ are determined by that of $\Psi_a(t)$, and the transients of $I_a^{AC}(t)$ and $I_f^{DC}(t)$ by that of $\Psi_f(t)$. We will now discuss the initial and transient states of $I_a^{DC}(t)$ and $I_f^{AC}(t)$ and those of $I_a^{AC}(t)$ and $I_f^{DC}(t)$ apart from each other.

5-2. Initial and Transient States of $I_a^{DC}(t)$ and $I_f^{AC}(t)$

Since $\Psi_a(0)=L_{md}I_f=E_0/\omega$ (See Eq.(19).), $I_a^{DC}(0)$ and $I_f^{AC}(0)$ are given by

$$\left.\begin{aligned} I_a^{DC}(0)&=\sqrt{\frac{2}{3}}\,\frac{1}{2}\left(\frac{1}{x'_d}+\frac{1}{x_q}\right)E_0\\ I_f^{AC}(0)&=\frac{kL_{md}}{L'_d}I_f=\frac{x_d-x'_d}{x'_d}I_f\end{aligned}\right\} \tag{25}$$

Although Eq.(25) agrees with the one obtained by the linear theory[5], x_d and x'_d,

---

* If all of the coefficients in Eq.(18) are constant, the solution is given by

$$\Psi_f(t)=\frac{E_0}{k\omega}\left\{\left(1-\frac{x'_d}{x_d}\right)e^{-t/T'_d}+\frac{x'_d}{x_d}\right\};\quad T'_d=\frac{L_fx'_d}{r_fx_d}.$$

in the present paper, are not constant but depend on I_f. Since $\Psi_a(t)$ decreases exponentially (See Eq.(20).), $I_a^{DC}(t)$ and $I_f^{AC}(t)$ also decrease exponentially. After all, what is to be noted about $I_a^{DC}(t)$ and $I_f^{AC}(t)$ is that although their initial values are influenced by the saturation, their transients are not.

Fig. 9 ~Fig. 11 show the theoretical values (full line) and the experimental values (circle) of $I_a^{DC}(0)$, $I_f^{AC}(0)$ and T_a, respectively. Eq.(20) and Eq.(25) were used for calculating the theoretical values. E_0, x_d and x'_d in the equations are obtained from the no-load saturation curve, Eq.(9) and Fig. 8 respectively. Other constants are $x_q=5.6\Omega$ (69%) and $r_a=0.22\Omega$ (2.7%). The experimental values are readings from an oscillograph. For reference, the characteristics, when x'_d is kept at the unsaturated value 2.3Ω (29%), are also shown by the broken line. The theoretical and experimental values agree well with each other.

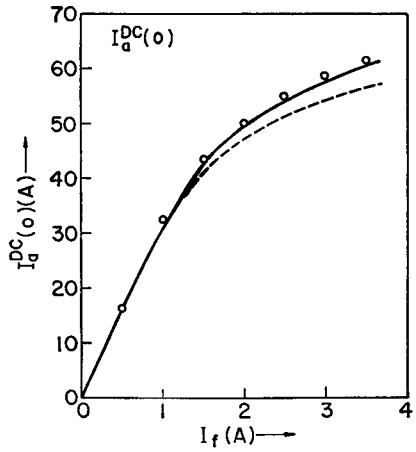

Fig. 9. Initial value of the direct-current component of armature-current.

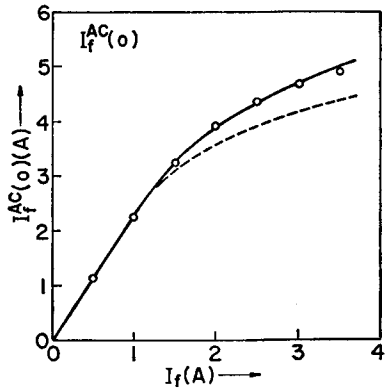

Fig. 10. Initial value of the alternating-current component of field-current.

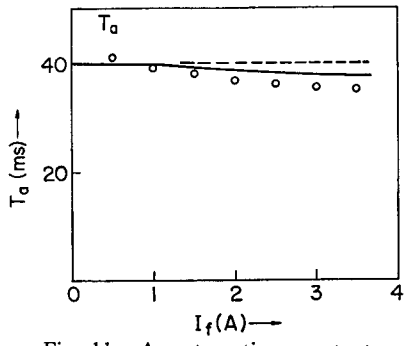

Fig. 11. Armature time-constant.

5-3. Initial and Transient States of $I_a^{AC}(t)$ and $I_f^{DC}(t)$

Since $\Psi_f(0)=L_fI_f=E_0/k\omega$ (See Eq.(19).), $I_a^{AC}(0)$ and $I_f^{DC}(0)$ are given by

$$I_a^{AC}(0)=\frac{1}{\sqrt{3}}\frac{E_0}{x'_d},\quad I_f^{DC}(0)=\frac{x_d}{x'_d}I_f \tag{26}$$

Although Eq.(26) agrees with the one obtained by the linear theory[5], x_d and x'_d in the present paper depend on I_f. Fig. 12 and Fig. 13 show $I_a^{AC}(0)$ and $I_f^{DC}(0)$. The theoretical and experimental values are obtained in the same way as in Fig. 9 and Fig. 10. The broken lines show the characteristics when the saturation of

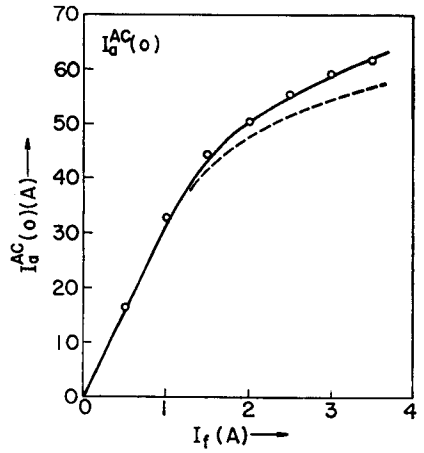

Fig. 12. Initial value of the alternating-current component of armature-current.

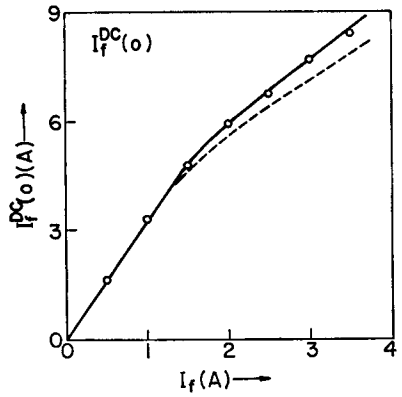

Fig. 13. Initial value of the direct-current component of field-current.

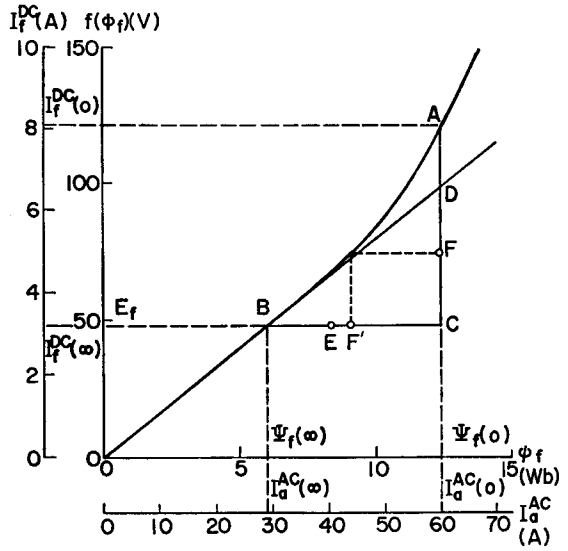

Fig. 14. Non-linear term $f(\psi_f)$ of Eq. (18).

x'_d is ignored.

In order to investigate the transient states of $I_a^{AC}(t)$ and $I_f^{DC}(t)$, let us consider Eq.(18) which dominates ψ_f. Fig. 14 shows the non-linear term of Eq.(18): $f(\psi_f)$ for $I_f=3.2$A. According to Eq.(18) and Eq.(24), $I_a^{AC}(t)$ is proportional to $\Psi_f(t)$ and $I_f^{DC}(t)$ is equal to $f(\Psi_f(t))/r_f$. Therefore, scales for $I_a^{AC}(t)$ and $I_f^{DC}(t)$ are also added to the figure. The initial value $\Psi_f(0)$ of ψ_f is given by $L_f I_f$ and its final value $\Psi_f(\infty)$ is determined by $f(\psi_f)-E_f=0$ $(E_f=r_f I_f)$. The initial and final values of $I_a^{AC}(t)$ and $I_f^{DC}(t)$ are also determined as shown in Fig. 14. Since the decreasing rate of ψ_f i.e. $-d\psi_f/dt$ is equal to $f(\psi_f)-E_f$ because of Eq.(18), the length between $\overset{\frown}{AB}$ $(f(\psi_f))$ and $\overline{BC}$ (E_f) in Fig. 14 represents the decreasing rate. If there is no saturation, the rate corresponds to the length between $\overline{BD}$ and $\overline{BC}$, and ψ_f decreases exponentially as the linear theory indicates[5]. Consequently, the following two features are pointed out about the saturation effects on the transients of $I_a^{AC}(t)$ and $I_f^{DC}(t)$.

(1) With regard to " Non-exponential decreasing ", Fig. 15 shows the variation of $I_f^{DC}(t)-I_f^{DC}(\infty)$ with logarithmic scales in both the unsaturated condition $(I_f=1.0\text{A})$ and the saturated condition $(I_f=3.2\text{A})$. The full lines represent simulation results by means of Eq.(18) and Eq.(24) where L_d and L_f are calculated by Eq.(14), L'_d by Fig. 8 and $r_f=15\Omega$. The circles show the measured values. Fig. 15 clarifies that $I_f^{DC}(t)-I_f^{DC}(\infty)$ varies exponentially in an unsaturated condition but varies non-exponentially in an saturated condition. Variation of $I_a^{AC}(t)-I_a^{AC}(\infty)$ has the same tendency as that of Fig. 15.

(2) As for " Faster transient variation ", in order to clarify quantitatively the

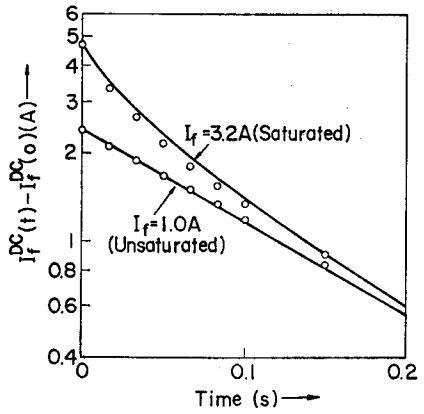

Fig. 15. Non-exponential decrease of the direct-current component of field-current.

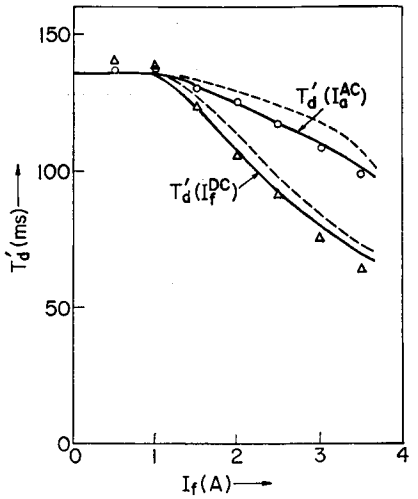

Fig. 16. Time-constants of I_a^{AC} and I_f^{DC}.

rate of the variation, let us define the time-constants of $I_a^{AC}(t)$ and $I_f^{AC}(t)$ in the same way as for the ordinary linear theory[5]. That is, the time-constant of $I_a^{AC}(t)$ is defined as the time when $I_a^{AC}(t)-I_a^{AC}(\infty)$ becomes equal to $[I_a^{AC}(0)-I_a^{AC}(\infty)]/e$, and is denoted by $T'_d(I_a^{AC})$. $T'_d(I_f^{DC})$ for $I_f^{DC}(t)$ is also defined similarly.

Fig. 16 shows $T'_d(I_a^{AC})$ and $T'_d(I_f^{DC})$, where the full lines show the simulated values of Eq.(18) and Eq.(24), while the circles and triangles are measured values. The broken lines show the characteristics when the saturation of x'_d is not considered. Not only does the time-constant become smaller as the saturation strengthens, but $T'_d(I_a^{AC})$ and $T'_d(I_f^{DC})$ are not equal to each other. $T'_d(I_a^{AC})$ is larger than $T'_d(I_f^{DC})$. The reason can be explained by Fig. 16 as follows.

Points E and F in the figure are such that CE: EB=AF: FC=$(1-1/e)$: $1/e$. $T'_d(I_a^{AC})$ and $T'_d(I_f^{DC})$ are equal to the times when $I_a^{AC}(t)$ and $I_f^{DC}(t)$ have the values represented by the points E and F respectively. Point F′ is the projection of F onto the ψ_f-axis. Hence, it follows that the relative positions of E and F′ lead to $T'_d(I_a^{AC})>T'_d(I_f^{DC})$.

As stated so far, magnetic saturation gives great effects on the transient states of the short-circuit currents.

Now, we want to emphasize that the saturation effects have been understood clearly by using a generator equation featuring flux-linkages as Eq. (17) and Eq.(18). In the conventional linear theory, the equation is usually written in terms of currents (i_d, i_q and i_f). However, in a non-linear analysis such as given in the present paper, writing the equation in terms of the currents not only leads to complicated forms of equations, but also makes it impossible to separate the equation into a linear part and a non-linear part.

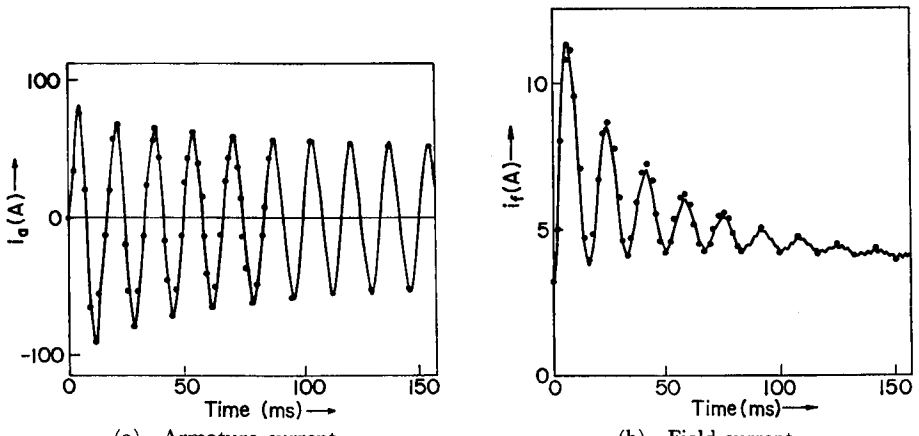

(a) Armature-current (b) Field-current

Fig. 17. Waveforms of short-circuit currents (I_f=3.2 A, E_0=220 V, α=100°).

5-4. Waveforms of Short-Circuit Currents

Fig. 17 shows measured (full line) and simulated (dots) waveforms of short-circuit currents for $I_f=3.2$A or $E_0=220$V. The simulation was carried out for Eq.(16) ~Eq.(18). The two waveforms satisfactorily agree with each other. This proves the validity of the discussions in the present paper.

6. Conclusion

In the present paper, the saturation effects on a sudden 3-phase short-circuit have been investigated in a case in which the saturation occurs primarily in the pole-core of a generator.

The results are summarized as follows.

(1) A direct-axis saturation model is easily derived from an equivalent circuit featuring a field flux-linkage.

(2) A generator equation featuring flux-linkages can be separated into a linear differential equation which regulates the armature flux-linkage, and a non-linear differential equation which regulates the field flux-linkage.

(3) Both the direct-current component of the armature-current and the alternating-current component of the field-current are regulated by the armature flux-linkage. Therefore, although their initial values are influenced by the saturation, their transient variations are not. That is, the latter are exponential, or in other words, linear.

(4) Both the alternating-current component of the armature-current and the direct-current component of the field-current are regulated by the field flux-linkage. As a result, both their initial values and their transient variations are influenced by the saturation. They decrease non-exponentially. Their time-constants become smaller as the saturation strengthens and are not equal to each other.

The saturation effects in a subtransient condition and in the case of saturation occurring in the armature-core will be investigated later.

Acknowledgement

The authors are indebted to Prof. Takao Okada for his valuable advice and discussions, and to Dr. Junya Matsuki for his helpful advice. We also wish to express our thanks to Kyoichi Fujita, Takashi Hikihara and Yoshitaka Tomomura, who as post-graduates co-operated with the experiment.

References

1) For example, see Professional group of IEEJ on synchronous machines' reactances: " On the saturation of synchronous machines' reactances ", Technical report of IEEJ (part I), *No. 135* (1983-5) (in Japanese).

2) For example, see Harley, R.G., et al: " Comparative study of saturation method in synchronous machine models ", IEE Proc., *Vol. 127*, Pt.B, No. 1, p.1 (1980–1).
3) Crary, S.B.: " Equivalent reactance of synchronous machines ", AIEE Trans., *Vol. 53*, p.124 (1934–1) and " Discussion by L.A. Kilgore ", ibid, p.487 (1934–4).
4) Mikhail, S.L.: " Potier reactance for salient-pole synchronous machines ", AIEE Trans., *Vol. 69*, p.235 (1950–2).
5) Adkins, B., et al.: " The General Theory of Alternating Current Machines " (book), Chapman and Hall Ltd. (1975).